This full text paper was peer reviewed at the direction of IEEE Communications Society subject matter experts for publication in the IEEE ICC 2009 proceedings

Markov Chain Minimum Bit Error Rate Detection for Multi-Functional MIMO Uplink

S. Sugiura*, S. Chen† and L. Hanzo†

*,†School of ECS, University of Southampton, SO17 1BJ, UK, Tel: +44-23-8059-3125, Fax: +44-23-8059-4508
Email: {ss07r,sqc,lh}@ecs.soton.ac.uk, http://www-mobile.ecs.soton.ac.uk
*Toyota Central R&D Labs., Inc., Aichi, 480-1192, Japan, Tel: +81-561-71-7163, Fax: +81-561-63-5258
Email: sugiura@mosk.tytlabs.co.jp, http://www.tytlabs.co.jp/eindex.html

***Abstract*— In this paper, we introduce a novel Markov Chain (MC) representation aided Minimum Bit Error Rate (MBER) detection method that is applicable to an $\mathcal{M}$-QAM modulated SDM/SDMA uplink system. Compared to the conventional MBER scheme, the proposed MC-MBER scheme is capable of reducing the complexity imposed with the aid of its efficient detection candidate set generation assisted by the Markov chain process. Our performance results demonstrate that the MC-MBER Multi-User Detection (MUD) is capable of reducing the computational complexity by a factor of eight in comparison to the conventional MBER MUD in a rank-deficient system transmitting four 4-QAM uplink substreams with the aid of two receive antennas at the Base Station (BS), while achieving a BER performance comparable to that of the MBER MUD.**

I. Introduction

In order to meet the increasing demand for bandwidth-efficient mobile communication services, Multiple-Input Multiple-Output (MIMO) systems employing antenna arrays, such as Spatial Division Multiplexing (SDM) and Space Division Multiple Access (SDMA), have been extensively investigated [1], [2]. While SDMA aims for maximizing the number of users supported, the goal of SDM is that of maximizing the throughput of a single user. Because these two MIMO arrangements constitute similar techniques, it is a natural further development to combine the functions of SDM and SDMA.

Since the invention of turbo codes by Berrou *et al.* [3], iterative linear detection based on the Minimum Mean Square Error (MMSE) criterion and exploiting the *a priori* information gleaned from a second decoder component has been investigated in diverse receivers, such as for example multiuser detection (MUD) [4] and turbo equalization [5]. Although the MMSE detection criterion has been widely used for iterative MUDs, minimizing the MSE does not necessarily guarantee the direct minimization of the system's Bit Error Ratio (BER).

By contrast, the family of Minimum BER (MBER) detectors [6]-[11] was designed to directly minimize the BER, and hence it was shown to outperform the MMSE solution in the context of beamforming [6], Space-Time Equalization (STE) [7], CDMA [8], SDMA [9] and Soft-Input Soft-Output (SISO) iterative detectors [10], supporting either BPSK or QPSK modulation schemes [11]. It was also demonstrated that the MBER receiver has the capability of operating in rank-deficient scenarios, where the number of transmit antennas is higher than the number of receive antennas. However, the high BER performance of the MBER scheme is achieved at the cost of a high computational complexity, which may become particularly challenging in rapidly fading propagation environments, requiring prompt MBER detector weight updates or in iterative detection scenarios, where soft information has to be exchanged between the detector and the channel decoder.

Recent studies of Markov chain simulations have found reduced-complexity applications in wireless communication systems [12]-[15]. The non-linear Markov Chain Monte Carlo (MCMC) based detector was designed for low-complexity near-optimum MUD [12]. The concept of the MCMC detector is based on the efficient extraction of the desired statistical inferences with the aid of Markov chains.

The financial support of the EU under the auspices of the Optimix project and also that of the EPSRC is thankfully acknowledged.

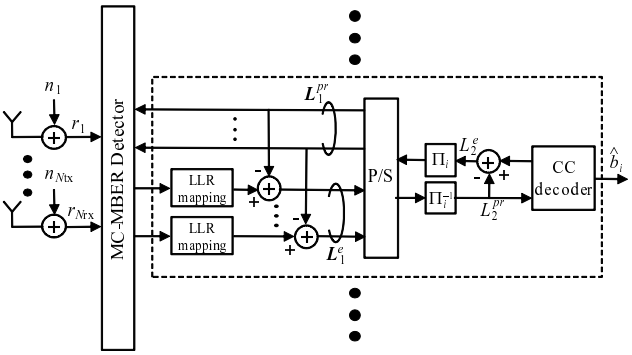

Fig. 1. Iterative receiver structure of a SDM/SDMA uplink.

Against this background, the novel contribution of this paper is that an MCMC aided MBER algorithm is proposed for the sake of reducing the computational complexity of the conventional MBER algorithm without degrading its performance. The BER performance and the computational complexity of the proposed MC-MBER detector are analyzed in the context of the rank-deficient 4-QAM and the 16-QAM SDM/SDMA uplink.

The remainder of this contribution is organized as follows. Section II describes the system model of our uplink scheme. The MC-MBER soft interference cancellation aided Multi-User Detection (MUD) is presented in Section III. In Section IV we provide our simulation results, followed by our conclusions in Section V.

II. System Overview

A. System Description

Consider a SDM/SDMA uplink scenario, where each of the $N_{\rm u}$ users has $N_{\rm tx}$ transmit antennas, while the Base Station (BS) is equipped with an $N_{\rm rx}$-element antenna array. At the ith user, the source bits b_i are first channel encoded and then interleaved by the user-specific interleaver Π_i. Next, the interleaved bits are S/P converted to $N_{\rm tx}$ substreams and then mapped to the $\mathcal{M}$-QAM symbols $\boldsymbol{s}_i = [s_i^{(1)}, \cdots, s_i^{(N_{\rm tx})}]^T$. Finally, a total of $N_{\rm u}N_{\rm tx}$ $\mathcal{M}$-QAM symbols are simultaneously transmitted via each transmit antenna of each user. For simplicity, we assume perfectly synchronous transmissions of all the users, which would require accurate adaptive timing advance control.

The structure of the iterative detection assisted receiver is shown in Fig. 1. Based on the turbo detection principle, the receiver employs an iterative MUD in the SDM/SDMA uplink. The receiver consists of two Soft-Input Soft-Output (SISO) stages, namely the SISO interference cancellation aided MUD and N_u number of parallel single-user

978-1-4244-3435-0/09/$25.00 ©2009 IEEE

SISO channel decoders. The MUD scheme employed demodulates the received symbols $\boldsymbol{r}$ and outputs the extrinsic information $\boldsymbol{L}_1^e$ in the form of Log Likelihood Ratios (LLRs) with the aid of the *a priori* LLRs $\boldsymbol{L}_1^{pr}$, which are fed back from the channel decoders to the detector. The extrinsic LLRs $\boldsymbol{L}_1^e$ are then input to the Convolutional Channel (CC) decoders of Fig. 1 after deinterleaving. The extrinsic LLRs L_2^e of Fig. 1 are calculated at the channel decoders, output and are interleaved again, before being passed back to the MUD component as the *a priori* information.

B. Signal Model

Assuming a frequency-flat channel environment, the received signals $\boldsymbol{r} \in \mathcal{C}^{N_{\rm rx}\times 1}$ are given by the complex-valued expression of

$$\boldsymbol{r} = \boldsymbol{H}\boldsymbol{s} + \boldsymbol{n}, \tag{1}$$

where $\boldsymbol{s} = [\boldsymbol{s}_1^T \cdots \boldsymbol{s}_{N_{\rm u}}^T]^T \in \mathcal{C}^{N_{\rm u}N_{\rm tx}\times 1}$ are the $\mathcal{M}$-QAM symbols and $\boldsymbol{n} \in \mathcal{C}^{N_{\rm rx}\times 1}$ are the corresponding noise components having a zero mean and a power of $2\sigma_n^2$. Furthermore, $\boldsymbol{H} \in \mathcal{C}^{N_{\rm rx}\times N_{\rm tx}}$ denotes the channel matrix.

Considering the MBER and MC-MBER schemes, it is convenient to represent the estimated signals by real-valued binary expressions. Let us hence consider the transformation of the complex-valued $\mathcal{M}$-QAM signal model (1) to the equivalent real-valued binary signal model.

Let us assume first of all that the ith user's and the lth antenna's $\mathcal{M}$-QAM symbol $s_i^{(l)}$ as well as the equivalent real-valued binary symbols $\tilde{\boldsymbol{b}}_i^{(l)} \in \mathcal{R}^{\log_2(\mathcal{M})\times 1}$ have the relationship of $s_i^{(l)} = \boldsymbol{q}\tilde{\boldsymbol{b}}_i^{(l)}$, where

$$\boldsymbol{q} = \begin{cases} \begin{bmatrix} 1/\sqrt{2} & -j/\sqrt{2} \end{bmatrix} & (\mathcal{M}=4) \\ \begin{bmatrix} 2/\sqrt{10} & 1/\sqrt{10} & -2j/\sqrt{10} & -j/\sqrt{10} \end{bmatrix} & (\mathcal{M}=16). \end{cases}$$

Then, the equivalent real-valued binary signal model is given by [16]

$$\boldsymbol{y} = \boldsymbol{H}'\boldsymbol{x} + \boldsymbol{\eta} \tag{2}$$

where we have

$$\boldsymbol{y} = [\Re(\boldsymbol{r})^T \ \Im(\boldsymbol{r})^T]^T \quad \in \mathcal{R}^{N\times 1}, \tag{3}$$
$$\boldsymbol{\eta} = [\Re(\boldsymbol{n})^T \ \Im(\boldsymbol{n})^T]^T \quad \in \mathcal{R}^{N\times 1}, \tag{4}$$
$$\boldsymbol{x} = [\bar{\boldsymbol{b}}_1^T \cdots \bar{\boldsymbol{b}}_{N_{\rm u}}^T]^T \quad \in \mathcal{R}^{M\times 1}, \tag{5}$$
$$\boldsymbol{H}' = [\Re(\boldsymbol{H}\boldsymbol{Q})^T \ \Im(\boldsymbol{H}\boldsymbol{Q})^T]^T \quad \in \mathcal{R}^{N\times M}, \tag{6}$$

with $M = N_{\rm u}N_{\rm tx}\log_2(\mathcal{M}), N = 2N_{\rm rx}$, $\bar{\boldsymbol{b}}_i = [\tilde{\boldsymbol{b}}_i^{(1)T} \cdots \tilde{\boldsymbol{b}}_i^{(N_{\rm tx})T}]^T$ and $\boldsymbol{Q} = \boldsymbol{I}_M \otimes \boldsymbol{q} \in \mathcal{C}^{M\times M\log_2(\mathcal{M})}$. Note that the equivalent real-valued noise components $\boldsymbol{\eta}$ have the power of $\sigma_n'^2 = \sigma_n^2$. Throughout the rest of this paper, we employ this real-valued signal model.

III. Markov Chain MBER Detection

In this section we first introduce the conventional MBER scheme, which outputs soft information. Then, we propose our detection algorithm and quantify the computational complexity of the detector.

A. Conventional MBER Detection

Let us define the $N_b = 2^M$ number of legitimate transmitted sequences of $\boldsymbol{x}$ as $\boldsymbol{x}^{(q)}$ $(q = 1, \cdots N_b)$, with $M = N_{\rm u}N_{\rm tx}\log_2(\mathcal{M})$. Then the error probability of the mth substream signal x_m can be expressed as [10]

$$P_e(\boldsymbol{w}_m) = \sum_{q=1}^{N_b} P(\boldsymbol{x}^{(q)}) \cdot Q\left[\frac{\mathrm{sgn}\left(\Re[x_m^{(q)}]\right)\cdot \check{x}_m^{(q)}}{\sigma_n'\sqrt{\boldsymbol{w}_m^H\boldsymbol{w}_m}}\right] \tag{7}$$

with

$$\check{x}_m^{(q)} = \Re[\boldsymbol{w}_m^H(\boldsymbol{H}'\boldsymbol{x}^{(q)} - \boldsymbol{H}'\bar{\boldsymbol{x}} + \bar{x}_m\boldsymbol{h}_m')], \tag{8}$$

where $P(\boldsymbol{x}^{(q)}) = \Pi_m P(x_m = x_m^{(q)})$ is the *a priori* probability of transmitting $\boldsymbol{x}^{(q)}$, and $Q[\,]$ is the Gaussian Q-function. Furthermore, the soft estimates $\bar{\boldsymbol{x}} = [\bar{x}_1 \cdots \bar{x}_M]^T$ are computed from the *a priori* LLRs $\boldsymbol{L}_1^{pr} = [L_{1,x_1}^{pr} \cdots L_{1,x_M}^{pr}]^T$ as

$$\bar{x}_m = \tanh(L_{1,x_m}^{pr}/2). \tag{9}$$

The MBER weights are derived by minimizing the BER function of (7) as follows

$$\boldsymbol{w}_{m,mber} = \arg\min_{\boldsymbol{w}} P_e(\boldsymbol{w}_m). \tag{10}$$

In (7) the probability $P_e(\boldsymbol{w}_m)$ is a nonlinear function of the weights $\boldsymbol{w}_i$, therefore in general the optimization problem has to be solved iteratively. Since the gradient of (7) is given by [10]

$$\nabla P_e(\bar{\boldsymbol{w}}_m) = \frac{1}{\sqrt{2\pi}\sigma_n'}\sum_{q=1}^{N_b} P(\boldsymbol{x}^{(q)})\exp\left(-\frac{(\check{x}_m)^2}{2\sigma_n'^2}\right)$$
$$\cdot\mathrm{sgn}(x_m^{(q)})\cdot\left(\bar{\boldsymbol{w}}_m\check{x}_m^{(q)} - (\boldsymbol{H}'\boldsymbol{x}^{(q)} - \boldsymbol{H}'\bar{\boldsymbol{x}} + \bar{x}_m\boldsymbol{h}_m')\right) \tag{11}$$

with $\bar{\boldsymbol{w}}_m = \boldsymbol{w}_m/\sqrt{\boldsymbol{w}_m^H\boldsymbol{w}_m}$, the Simplified Conjugate Gradient (SCG) algorithm [6] provides an efficient solution for this optimization problem. As described in [10], the real part of the symbols estimated by the MBER detector is non-Gaussian. Thus, the exact expression of the extrinsic information has to be employed, which is given by

$$L_{1,x_m}^e = \ln\frac{\sum_{x_m^{(q)}=0} P(\hat{x}_m|\boldsymbol{x}^{(q)})\Pi_{m'\neq m}P(x_{m'}^{(q)})}{\sum_{x_m^{(q)}=1} P(\hat{x}_m|\boldsymbol{x}^{(q)})\Pi_{m'\neq m}P(x_{m'}^{(q)})}, \tag{12}$$

where we have:

$$P(\hat{x}_m|\boldsymbol{x}^{(q)}) = \frac{1}{\sqrt{2\pi}\sigma_n'}\exp\left(-\frac{\Re^2\left[\bar{\boldsymbol{w}}_m^H(\boldsymbol{y} - \boldsymbol{H}'\boldsymbol{x}^{(q)})\right]}{2\sigma_n'^2}\right) \tag{13}$$

$$P(x_{m'}^{(q)}) = \left[1 + \mathrm{sgn}(x_{m'}^{(q)})\tanh(L_{1,x_m}^{pr}/2)\right]/2. \tag{14}$$

Clearly, the calculation of the MBER weight gradient in (11) imposes a high computational complexity, which increases exponentially with the value of M. It may be readily shown that an unlikely signal set of $\boldsymbol{x}^{(q)}$ resulting in a small value of $P(\boldsymbol{x}^{(q)})$ does not substantially contribute to the gradient expression of (11). Thus, we introduce the Markov Chain (MC) representation method that efficiently extracts a likely set of signals from the $N_b = 2^M$ legitimate sequences for the sake of reducing the computational complexity associated with the gradient calculation in (11) without degrading the BER performance of the full-complexity MBER scheme.

B. Principle of Markov Chain MBER Detection

The MCMC algorithm [12]-[15] is based on two different techniques, i.e. MC representation and Monte Carlo integration. While the former is employed to find the most likely detection candidates according to the associated probability distributions, the latter is used to approximate the integral of interest on the basis of the detection candidates calculated by the Markov chain representation. In our MC-MBER detector, only the MC representation is used to generate the most likely $N_b' < N_b$ number of signals $\boldsymbol{x}^{(q')}$ (q'=1, $\cdots$, N_b'), which are our detection candidates in this paper. The detection candidates are then input to the MBER detector.

Several algorithms have been designed for finding the most likely decision candidate set with the aid of a MC process [14]. In this contribution we employ the most popular so-called Gibbs-Sampler, which assists us in sampling the detection candidates set, with the aim of finding the most likely ones [15]. Fig. 2 portrays a flowchart of

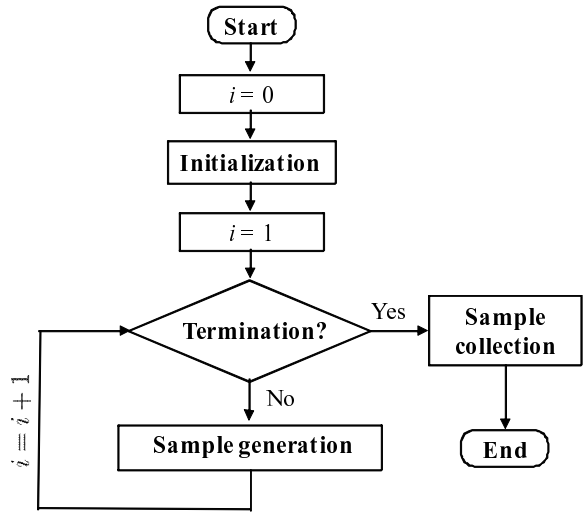

Fig. 2. A flowchart depicting the structure of Gibbs-Sampler used in the SDM/SDMA system.

the Gibbs-Sampler algorithm employed in our SDM/SDMA system, where the algorithmic steps are as follows:

1) *Initialization:* The initialization block of the Gibbs-Sampler of Fig. 2 randomly generates binary signals $\boldsymbol{x}[i=0] = [x_1[0]\cdots x_M[0]]^T$, which represent one of the $N_b = 2^M$ legitimate signal sequences of (5) in our $\mathcal{M}$-QAM SDM/SDMA system.
2) *Sample Generation:* In the sample generation block of Fig. 2, the signals $\boldsymbol{x}[i] = [x_1[i]\cdots x_M[i]]^T$ generated during the ith loop are calculated based on the $(i-1)$st signals $\boldsymbol{x}[i-1]$, on the *a priori* LLRs $\boldsymbol{L}_1^{pr}$, on the received signals $\boldsymbol{y}$ and on the estimated channels $\boldsymbol{H}'$. To be more specific, the mth element $x_m[i]$ of the signals $\boldsymbol{x}[i]$ is sampled from the conditional probability [15]

$$P(x_m = +1|\boldsymbol{x}_{-m}, \boldsymbol{y}, \boldsymbol{L}_1^{pr}) = 1/\left(1 + \frac{P(x_m=-1,\boldsymbol{x}_{-m}|\boldsymbol{L}_1^{pr})p(\boldsymbol{y}|x_m=-1,\boldsymbol{x}_{-m})}{P(x_m=+1,\boldsymbol{x}_{-m}|\boldsymbol{L}_1^{pr})p(\boldsymbol{y}|x_m=+1,\boldsymbol{x}_{-m})}\right) \quad (15)$$

with

$$p(\boldsymbol{y}|x_m = \pm 1, \boldsymbol{x}_{-m}) = \frac{1}{(\sqrt{2\pi}\sigma_n')^N} \exp\left(-\frac{||\boldsymbol{y} - \boldsymbol{H}'\tilde{\boldsymbol{x}}||^2}{2\sigma'^2}\right), \quad (16)$$

where we have $\boldsymbol{x}_{-m} = [x_1[i], \cdots, x_{m-1}[i], x_{m+1}[i-1], \cdots, x_M[i-1]]^T$ and $\tilde{\boldsymbol{x}} = [x_1[i], \cdots, x_{m-1}[i], x_m, x_{m+1}[i-1], \cdots, x_M[i-1]]^T$. When a real-valued random variable ζ, which is uniformly distributed between 0 and 1, happens to be lower than the probability $P(x_m = +1|\boldsymbol{x}_{-m}, \boldsymbol{y}, \boldsymbol{L}_1^{pr})$, the mth element $x_m[i]$ is set to $+1$, otherwise, to -1. This sample generation block is activated for N_s iterations, thus a total of N_s signals $\boldsymbol{x}[i]$ $(i = 1, \cdots, N_s)$ are generated.
3) *Sample Collection:* Finally, in the sample collection block, the signals generated in the last $N_{\rm MC}$ iterations are collected as the most likely detection solutions identified by the Gibbs-Sampler. Here, the first $N_{\rm burn} = N_s - N_{\rm MC}$ iterations are selected as the *burn-in* period indicating that these initial detection candidates are typically discarded, which allows the solution to converge at the most likely values from the randomly generated initial solutions $\boldsymbol{x}[0]$.

It is clear that the $N_{\rm MC}$ number of detection candidates generated by the Gibbs-Sampler of Fig. 2 are mutually correlated since all of the signals are originated from the initial conditions $\boldsymbol{x}[0]$. Therefore, $N_{\rm P}$ parallel Gibbs-Samplers may be invoked to avoid the problem of having highly correlated successive Gibbs-Sampler solutions [14]. The employment of this method results in an increased number of detection candidates $N_{\rm MC}N_{\rm P}$.

Having completed the generation of the Gibbs-Sampler's detection candidate set of $N_{\rm MC}N_{\rm P}$ signals, only $N_b' < N_b$ number of detection candidates $\boldsymbol{x}^{(q')}$ are retained from the Gibbs-Sampler solution set, also ensuring that the identical detection candidates of the parallel Gibbs-Samplers are removed. Then, these $N_b' < N_b$ detection candidates are used for calculating the gradient in (11) by replacing N_b and $\boldsymbol{x}^{(q)}$ by $N_b' < N_b$ and $\boldsymbol{x}^{(q)'}$, respectively. Typically, N_b' becomes significantly lower than $N_b = 2^M$, which is an explicit benefit of the rapid convergence of the Gibbs-Sampler detailed in Fig. 2.

Broadly speaking, the computational complexity of the MC-MBER detector, which is required for calculating the gradient of the BER with respect to the weights in (11), can be reduced by a factor of N_b/N_b' in comparison to that of the full-complexity MBER scheme, although the MC-MBER detector imposes the additional computation of the Gibbs-Sampler based reduced set of $N_b' < N_b$ signals.

The total computational complexity of the MMSE, the MBER, and the MC-MBER detectors is listed in Table I, where N_∇ is the number of iterations activated by the simplified conjugate algorithm used for finding the minimum of the BER versus MBER detector weight surface. More explicitly, the number of real-valued additions, multiplications and the exponential value calculations are listed in Table. I.

TABLE I
COMPUTATIONAL COMPLEXITY OF THE MMSE, MBER AND MC-MBER DETECTORS

MUD		Computational complexity	
MMSE	$\boldsymbol{w}$	additions:	$4MN^2 + 6N^2 - N$
		multipl.:	$4MN^2 + 2MN + 10N^2$
		inverse:	$\mathcal{O}(N^3)$
	$\boldsymbol{L}_1^e$	addition:	$2MN + 6N - 1$
		multipl.:	$2MN + 6N + 2$
MBER	$\boldsymbol{w}$	additions:	$N_\nabla(3NN_b + 4MN - 2M + 7N - 2) + (2MN + 4M + 4N - 2)N_b$
		multipl.:	$N_\nabla[(3N+4)N_b + 4MN + 13N + 3] + (4MN + 4N)N_b$
		exp.:	$N_\nabla N_b$
	$\boldsymbol{L}_1^e$	additions:	$(3MN + 2N + 1)N_b - 2$
		multipl.:	$(4MN + M + 2N + 5)N_b + 1$
		exp.:	$N_b + 1$
MC-MBER	$\boldsymbol{w}$	additions:	$N_\nabla(3NN_b' + 4MN - 2M + 7N - 2) + (2MN + 4M + 4N - 2)N_b' + N_{\rm P}(N_{\rm burn} + N_{\rm MC}) \times M(8MN + 6N) + 1$
		multipl.:	$N_\nabla[(3N+4)N_b' + 4MN + 13N + 3] + (4MN + 4N)N_b' + N_{\rm P}(N_{\rm burn} + N_{\rm MC}) \times M(8MN + 8N + 4) + 1$
		exp.:	$N_\nabla N_b' + N_{\rm P}(N_{\rm burn} + N_{\rm MC})M$
	$\boldsymbol{L}_1^e$	additions:	$(3MN + 2N + 1)N_b - 2$
		multipl.:	$(4MN + M + 2N + 5)N_b + 1$
		exp.:	$N_b + 1$

TABLE II
BASIC SYSTEM PARAMETERS

Number of users N_u	2
Number of Tx antennas N_{tx}	2
Number of Rx antennas N_{rx}	2
Modulation Scheme	4-QAM
Channel	Frequency flat Rayleigh fading channel
Outer channel code	RSC (2,1,5) with generator polynomials $(35, 23)_8$
Interleaver block length	200,000 bits
Number of Iterations I	I = 0 to 7
RSC Channel decoder	Approximate Log MAP
Weight optimization criterion	MMSE, MBER and MC-MBER
Burn-in period N_{burn}	5
Number of signals generated in a single Gibbs-Sampler N_{MC}	10
Number of parallel Gibbs-Samplers N_P	1, 5
Number of iterations in the SCG algorithm N_∇	100

IV. PERFORMANCE ANALYSIS

In this Section, we present our performance results characterizing the proposed MC-MBER aided system employing N_{rx}=2 receive antennas at the BS and supporting $N_u = 2$ users having $N_{\mathrm{tx}} = 2$ transmit antennas, which results in the $(N \times M) = (4 \times 8)$-element equivalent channel matrix $\boldsymbol{H}'$. For comparison, the performance of the MMSE and MBER detectors is also considered. The basic system parameters are listed in Table II. Each user has a different random interleaver having a length of 200,000 bits and employs the same half-rate Recursive Systematic Convolutional (RSC) code having a constraint length of 5 and the octally represented generator polynomials of (35, 23). For each user, $N_{\mathrm{tx}} = 2$ number of 4-QAM modulated symbols are transmitted over frequency flat Rayleigh fading channels, where the total bandwidth efficiency is 4 bits/s channel use, corresponding to 4 bits/s/Hz in case of zero Nyquist access bandwidth.

A. BER performance

Fig. 3 demonstrates the achievable BER performance of the MC-MBER based MUD having different number of iterations spanning from I=0 to I=7. The parameters used for the Gibbs-Sampler were set to N_{burn}=5, N_{P}=1 and N_{MC}=10, respectively. Furthermore, the corresponding perfect cancellation based single-stream bound is also plotted in Fig. 3. It can be seen that the BER performance is substantially improved upon increasing the number of iterations I, reaching the perfect cancellation based single-stream bound at SNR = 3 dB in case of $I = 7$.

Fig. 4(a) shows the achievable BER performance of the MC-MBER detector in conjunction with both N_{P} = 1 and N_{P} = 5, as well as that of the MMSE and MBER detectors. The other parameters of the Gibbs-Sampler algorithm remained N_{burn}=5 and N_{MC}=10. The MC-MBER curves of both N_{P} = 1 and N_{P} = 5 exhibit good BER results, which are close to that of the full-complexity MBER detector, while MMSE detector exhibits 4 dB worse performance at the BER of 10^{-5} in this challenging rank-deficient scenario. It can be also concluded that the MC-MBER detector's performance in this simulation is essentially unaffected by the number of parallel chains N_{P}. This is owing to the fact that the MC-MBER is capable of directly reducing the BER, as far as the N_b' number of detection candidates includes the transmitted signals to be detected. This is beneficial in terms of reducing the computational complexity imposed, since the total number of parallel chains is reduced.

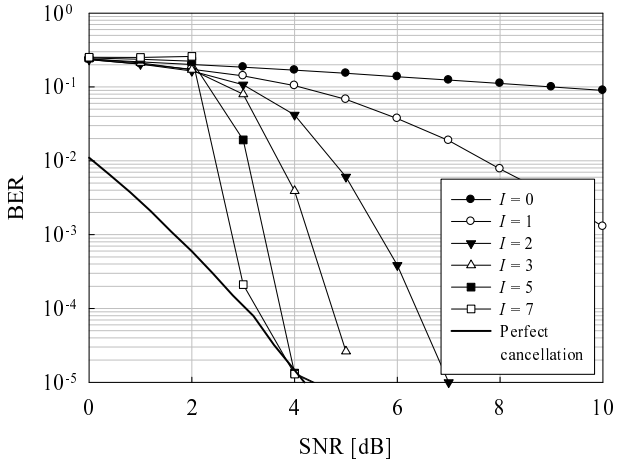

Fig. 3. BER performance of the MC-MBER detector having different number of iterations I in a 4-QAM SDM/SDMA scenario using $N_u = 2$, $N_{\mathrm{tx}} = 2$ and $N_{\mathrm{rx}} = 2$. The MC-MBER detector was configured to use N_{P}=1, i.e. a single, Markov chain having a burn-in period of $N_{\mathrm{burn}} = 5$ and $N_{\mathrm{MC}} = 10$ signals generated in a single Gibbs-Sampler.

TABLE III
COMPUTATIONAL COMPLEXITY EXPRESSED AS THE SUM OF REAL-VALUED ADDITIONS AND MULTIPLICATIONS AT SNR = 3 DB IN THE 4-QAM SDM/SDMA SYSTEM

MUD	Complexity			BER
	Gibbs-Sampler	SCG	Total	
MC-MBER, N_{P}=1	68,642	36,932	105,574	2.1×10^{-4}
MC-MBER, N_{P}=5	343,203	41,011	384,214	1.2×10^{-4}
MBER	—	813,924	813,924	1.0×10^{-4}

In addition to the 4-QAM system shown in Table II, we also investigated in Fig. 4(b) the achievable BER performance of a 16-QAM SDMA system employing N_{rx}=2 receive antennas at the BS and supporting $N_u = 2$ users, each having $N_{\mathrm{tx}} = 1$ transmit antenna. Although this 16-QAM system is not a rank-deficient one, both the proposed MC-MBER detectors using N_{P} = 1 and N_{P} = 5 exhibit a better performance than the MMSE detector, while reaching the single-user bound at SNR = 6 dB.

B. Computational Complexity

Fig. 5 shows the number of detection candidates N_b' used for calculating the gradient of the MC-MBER weights in (11), where the number N_b' was averaged over all the iterations I at each SNR. The number $N_b = 2^M = 2^8 = 256$ used for the full-complexity MBER scheme is also plotted in Fig 5. For the MC-MBER scheme, we had $N_b' < N_b$. More specifically, in case of N_{P} = 1, the number of detection candidates N_b' tended to be unity upon increasing the SNR. We also note that the 16-QAM system considered in Fig. 4(b) achieves a set-size reduction, where $N_b' < N_b$ similarly to the 4-QAM system.

Table III shows the computational complexity required to calculate the weights $\boldsymbol{w}_m$ for the full-complexity MBER and for the MC-MBER detectors at the SNR = 3 dB in our SDM/SDMA system. The complexity was evaluated in terms of the number of real-valued operations, expressed as the sum of real-valued multiplications

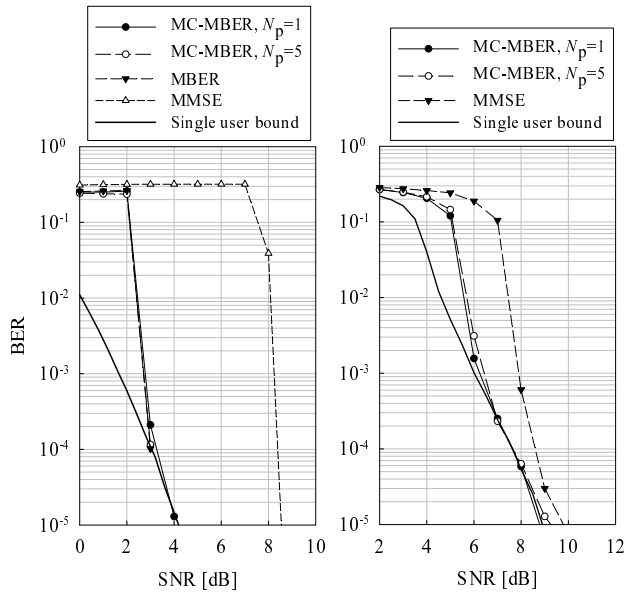

Fig. 4. BER performance of the MMSE, MBER and MC-MBER detectors using I = 7 iterations in (a) a 4-QAM SDM/SDMA scenario employing $N_u = 2$, $N_{\rm tx} = 2$ and $N_{\rm rx} = 2$ and in (b) a 16-QAM SDM/SDMA scenario employing $N_u = 2$, $N_{\rm tx} = 1$ and $N_{\rm rx} = 2$. The MC-MBER detector invoked $N_{\rm P}$=1 or $N_{\rm P}$=5 Markov chains having a burn-in period of $N_{\rm burn} = 5$ and $N_{\rm MC} = 10$ signals generated in a single Gibbs-Sampler.

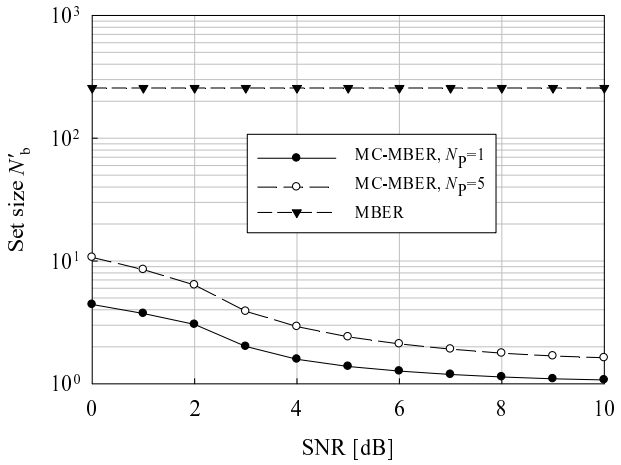

Fig. 5. Number of detection candidates N'_b generated by the Gibbs-Sampler, and used for calculating the gradient of the MC-MBER weights in (11), where N'_b was averaged over all the iterations I at each SNR. The value of $N_b = 2^M = 2^8 = 256$ used for the full-complexity MBER detector is also plotted.

and real-valued additions, although one may argue that a h-bit multiplication requires h shift-and-add operations and hence may be deemed h-times more complex. Furthermore, since the MC-MBER detector requires both the Gibbs-Sampler and the SCG algorithms, both their complexity is characterized as well as the total complexity in Table III. The total complexity of the MC-MBER detector using $N_{\rm P}$=1 was found to be a factor of eight lower than that of the full-complexity MBER scheme. Additionally, it is seen in both the MC-MBER detectors using both $N_{\rm P}$=1 and $N_{\rm P}$=5 that the Gibbs-Sampler constitutes the dominant factor in the total complexity in comparison to the SCG algorithm.

According to Table I, it is also anticipated that the complexity advantage of the MC-MBER scheme over the MBER scheme increases upon increasing M, since the number of detection candidates N'_b does not increase exponentially.

V. Conclusion

In this paper, we proposed a reduced-complexity Markov chain representation aided MBER detector designed for the SDM/SDMA uplink. Our simulation results revealed that the complexity of the MC-MBER MUD is a factor of eight lower than that of the MBER MUD in an 4-QAM modulated rank-deficient system having $N_{\rm rx}$=2 receive antennas and N_u=2 users, each employing $N_{\rm tx}$=2 receive antennas, while keeping the BER performance comparable to that of the MBER MUD.

References

[1] L. Hanzo, M. Münster, B. Choi, and T. Keller, *OFDM and MC-CDMA for Broadband Multi-User Communications, WLANs, and Broadcasting*. John Wiley and IEEE Press, 2003.

[2] L. Hanzo, O. Alamri, M. El-Hajjar, and N. Wu, *Near-Capacity Multi Functional MIMO Systems*. John Wiley and IEEE Press, 2009.

[3] C. Berrou, A. Glavieux, and P. Thitimajshima, "Near Shannon limit error-correcting coding and decoding: Turbo-codes." *IEEE International Conference on Communications, 1993, Geneva*, vol. 2, pp. 1064–1070.

[4] X. Wang and H. Poor, "Iterative (turbo) soft interference cancellation and decoding forcoded CDMA," *IEEE Transactions on Communications*, vol. 47, no. 7, pp. 1046–1061, 1999.

[5] M. Tüchler, A. Singer, and R. Koetter, "Minimum mean squared error equalization using a priori information," *IEEE Transactions on Signal Processing*, vol. 50, no. 3, pp. 673–683, 2002.

[6] S. Chen, A. Samingan, B. Mulgrew, and L. Hanzo, "Adaptive minimum-BER linear multiuser detection for DS-CDMA signals in multipath channels," *IEEE Transactions on Signal Processing*, vol. 49, no. 6, pp. 1240–1247, 2001.

[7] S. Chen, A. Livingstone, and L. Hanzo, "Minimum bit-error rate design for space-time equalization-based multiuser detection," *IEEE Transactions on Communications*, vol. 54, no. 5, pp. 824–832, 2006.

[8] J. Li, G. Wei, and F. Chen, "On minimum-BER linear multiuser detection for DS-CDMA channels," *IEEE Transactions on Signal Processing*, vol. 55, no. 3, pp. 1093–1103, 2007.

[9] S. Chen, L. Hanzo, and A. Livingstone, "MBER space-time decision feedback equalization assisted multiuser detection for multiple antenna aided SDMA systems," *IEEE Transactions on Signal Processing*, vol. 54, no. 8, pp. 3090–3098, Aug. 2006.

[10] S. Tan, S. Chen, and L. Hanzo, "On multi-user EXIT chart analysis aided turbo-detected MBER beamformer designs," *IEEE Transactions on Wireless Communications*, vol. 7, no. 1, pp. 314–323, 2008.

[11] S. Chen, L. Hanzo, N. Ahmad, and A. Wolfgang, "Adaptive minimum bit error rate beamforming assisted receiver for QPSK wireless communication," *Digital Signal Processing*, vol. 15, no. 6, pp. 545–567, 2005.

[12] Z. Yang, B. Lu, and X. Wang, "Bayesian Monte Carlo multiuser receiver for space-time coded multicarrier CDMA systems," *IEEE Journal on Selected Areas in Communications*, vol. 19, no. 8, pp. 1625–1637, 2001.

[13] R. Chen, J. Liu, and X. Wang, "Convergence analyses and comparisons of Markov chain Monte Carlo algorithms in digital communications," *IEEE Transactions on Signal Processing*, vol. 50, no. 2, pp. 255–270, 2002.

[14] A. Doucet and X. Wang, "Monte Carlo methods for signal processing: a review in the statistical signal processing context," *IEEE Signal Processing Magazine*, vol. 22, no. 6, pp. 152–170, 2005.

[15] B. Farhang-Boroujeny, H. Zhu, and Z. Shi, "Markov chain Monte Carlo algorithms for CDMA and MIMO communication systems," *IEEE Transactions on Signal Processing*, vol. 54, no. 5, pp. 1896–1909, 2006.

[16] H. Vikalo, B. Hassibi, and T. Kailath, "Iterative decoding for MIMO channels via modified sphere decoding," *IEEE Transactions on Wireless Communications*, vol. 3, no. 6, pp. 2299–2311, 2004.